North-Holland

Breakup of invariant tori for the four-dimensional semi-standard map

Erik M. Bollt and James D. Meiss
Program in Applied Mathematics, Box 526, University of Colorado, Boulder, CO 80309, USA

Accepted 25 January 1993

Explicit bounds on the domain for fixed k are obtained. Numerical results show that quadratic irrationals can be more

1. Introduction

Diophantine torus for any small enough pertur-

stroyed and can be made rigorous [16]. The

[illegible]

some cases using interval arithmetic) of the con-

[illegible]

Though many have attempted to generalize

[illegible]

more than two degrees of freedom, or equivalently, symplectic maps of four or more dimensions, there has been limited success in determin-

[illegible]

approximations to invariant tori have been obtained [14,25], and computations reveal that the

[illegible]

studies is number theoretic: there is no satisfac-

[illegible]

theory to simultaneous approximation of several irrationals

[illegible]

because their continued fraction expansions are eventually periodic (these give rise to self-similar structures). Finally, the most robust tori appear to correspond to the class of quadratic irrationals known as the noble numbers: these have a con-

[illegible]

Roughly speaking, the explanation for this is that

There has been some speculation that for four-

[illegible]

therefore cubic [11,12]. However, even in this

[illegible]

self-similar behavior near breakup [21], and there is no evidence that cubic irrationals are more robust than others.

[illegible]

complex, symplectic map corresponding to the coupling of two semi-standard maps is intro-

[illegible]

Fourier series for the semi-Froeschle map, we are

[illegible]

holomorphic functions of several complex vari-

[illegible]

2. Coupling of two semi-standard maps

The semi-standard area-preserving map was

[illegible]

numerically simpler model than the standard the semi-standard map takes $\{x_{t-1}, x_t\} \mapsto$

$$\delta^2 x_t \equiv x_{t+1} - 2x_t + x_{t-1} = \ldots \quad (1)$$

... this is a map ... the notation δ^2 is reminiscent of the second derivative operator.

In this paper we study a four-dimensional ...

... mapping is

$$F(x) \equiv \ldots \quad (3)$$

There are three parameters, the strength of the ... (a_1, a_2) and ϵ, the strength of the coupling of the two maps. Eq. (2) is symplectic since F is the gradient of a scalar potential (see for example [14]).

We are looking for solutions x of eq. (2) that ...

... torus be analytically conjugate to a uniform rota- ...

$$x_t \longrightarrow x_{t+1} \quad (4)$$

Thus, for a given ω, an invariant torus for eq. (2) is given by

$$x_t = x(\theta + 2\pi\omega t)\,, \quad (5)$$

... thus $x(\theta)$ is coperiodic with θ ...

$$x(\theta) = \theta + \chi(\theta)$$

where $\chi(\theta)$ is doubly 2π periodic. If we suppose ... Inserting eq. (5) into eq. (2) yields the Percival form of the mapping

$$\delta^2 x(\theta) = x(\theta + 2\pi\omega) - 2x(\theta) + x(\theta - 2\pi\omega) = F(x(\theta)) \quad (8)$$

... equations determining the Fourier coefficients χ_k; these will be obtained in section 4.

3. Incommensurate frequencies

... in [10,27,29]. In particular, rather sophisticated ... were developed in [27]; these give accurate ...

for which there is an analytic invariant circle with frequency ω. Here a^{ss}, the critical function, is ... zero for every rational ... value and exhibits a maximum for ...

The critical function appears to have a local maximum at each of the *noble frequencies*: those equivalent to γ under a modular transformation, or equivalently which have a continued fraction

These results also apply to the semi-Froeshlé map when $\epsilon = 0$. Thus an invariant torus of

KAM theory implies that for sufficiently small

quency vector satisfies a Diophantine condition.

tors $\mathcal{D}_\mu$ consists of those $\omega \in \mathbb{R}^d$ for which there exists a $C > 0$ such that for all $(p, q) \in \mathbb{Z}^{d+1}$

$$|p \cdot \omega - q| \geq \frac{C}{\|p\|^\mu}, \tag{11}$$

K

If $d = 1$ then K can be replaced by $1/\sqrt{5}$ but nothing smaller.

Diophantine are those constructed from alge-

Recall that an algebraic field generated by $\xi \in \mathbb{R}$ of degree n is defined as the set of numbers of the form

$$R(\xi) = \frac{P(\xi)}{\dots}$$

$$\sigma \in \sqrt{2} = [2, 2, 2, 2. \ldots] \equiv [2^\infty] ,$$

$$\zeta \equiv \frac{1+\sqrt{2}}{5+4\sqrt{2}} = [0, 4, 2^\infty] . \tag{13}$$

The expressions on the right hand sides above give the continued fraction expansions. Setting

easy to see, since $\xi^4 - 14\xi^2 + 9 = 0$ and any polynomial in ξ has the form $P(\xi) = a + b\sqrt{2} + c\sqrt{5} + d\sqrt{10}$ for $a, b, c, d \in \mathbb{Z}$. Thus γ, σ, and ζ

$$\tau^3 = \tau + 1 ,$$

$\tau \simeq$ 1.32 471 795 724 474 602 596 090 885 44…

5, 1, 2, 8, 2, 1, 1, 3, 1, . . .] . (14)

This so called "spiral mean" frequency was in-

elements appear unbounded [22]. None-the-less,

τ is the smallest of the "PV numbers", which

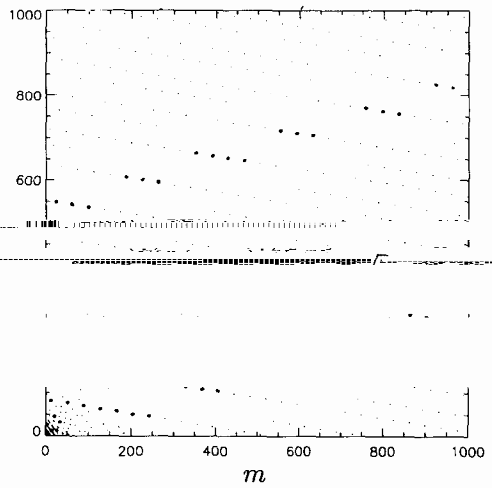

terms of the small denominators

$D_m \equiv 4 \sin^2(\pi m \cdot \omega)$ (15)

pect the Fourier coefficients to have similar isolated peaks

fortunately not the case.

our expansions. Further, using eq. (7) we define

$$g(u) = \mathrm{i}[x(\theta) - \theta] = \mathrm{i}\chi(\theta) . \quad (17)$$

be needed in the Fourier expansion of $\chi(\theta)$. $g(u)$ has a Taylor expansion

$$g(u) = \sum b_n u^n$$

Here we use standard multi-index notation for the vector exponentiation: while $u \in \mathbb{C}^2$ and $n \in \mathbb{N}^2$, $u^n = u_1^{n_1} u_2^{n_2} \in \mathbb{C}$. In addition to the expansion of g, we will need the expansions of its exponential as well:

$$\mathrm{e}^{g_i(u)} = \sum c_n^{(i)} u^n , \quad (19)$$

$$-k \left(u_1 u_2 \, \mathrm{e}^{g_1(u) + g_2(u)} \right) . \quad (20)$$

is the coupling parameter. Note that these coefficients

If ω is incommensurate, then D_n is nonzero, so

define the partial order $\leq$ on integer vectors by

A simple derivative identity allows us to find the coefficients

$$\frac{\mathrm{d}}{\mathrm{d}u_j} \mathrm{e}^{g_i(u)} = \left(\frac{\mathrm{d}}{\mathrm{d}u_j} g_i(u) \right) \mathrm{e}^{g_i(u)} \quad (23)$$

$$n_j c_n^{(i)} = \sum_{m \neq (0,0)}^{n} m_j b_m^{(i)} c_{n-m}^{(i)} \quad (24)$$

Note that eq. (24) allows the two forms, $j = 1$ or 2, for n off the axis (these are equivalent), but for n on the axis, only one is valid because of a examination of the mapping, eq. (25), yields in addition

$b^{(2)} = 0$, $b^{(1)} = 0$ (26)

... and ... are identical to those for the ... respectively.

... the domain of convergence of $g(u)$ is the ... each component's series.

$$S = \sum b_m z^m , \tag{28}$$

similar to the series obtained in the previous ...

projection onto the radius space is denoted Π:

Several types of subsets of $\mathbb{C}^d$ are of interest.

interior of the set of points for which it converges absolutely. A *polydisk* is the appropriate ... 1, ..., d}. A *Reinhardt domain* is a domain R such that ...

main is *complete* if for every $z \in R$ the polydisk ...

points with smaller radii. Finally a domain D is ...

is a convex subset of $\mathbb{R}^d$.

terms at a point z then it converges absolutely to a holomorphic function. The domain of convergence, D, of S is the interior of the set for which $|b_m z^m|$ is bounded. Furthermore D is a log...

ly, if $|b_m z^m|$ is unbounded then there is an order-...

Its most unusual aspect is that the domain of ...

in more detail. Suppose $z, x \in \mathbb{C}^{d*} \cap D$. Then for $\alpha + \beta = 1$ let u be any point in $\mathbb{C}^{d*}$ such that

where r_i and s_i are the radii of z and x, respec-

x. $B = \sup(|b_m z^m|, |b_m x^m|)$ exists, and straightforward since the series eq. (18) has the

Corollary 1. For fixed k defined by eq. (21), an analytic invariant torus with Diophantine fre-

function $r_1(r_2)$ or $r_2(r_1)$.

tion of these domains is possible with reasonable

6. Numerical results

they are real and positive for $n = 0$. The next

the ith component is

$$\log(r_1^{(i)}(s)) = -\lim_{n\to\infty} \frac{\log \ldots}{n} \quad (36)$$

for each fixed s. Since the domain of conver-

factor of ten in computing time over using the

lead us to choose $N = 255$ as our matrix di-

of the Fourier coefficients. We first consider $\omega = (\gamma, \sigma)$ where the components were defined by eqs. (10) and (13). Fig. 2 is a logarithmic

the recursion algorithm, which shows that b_m is a

jump. This can be seen in the contour plot as a

coefficients for greater m are influenced by this

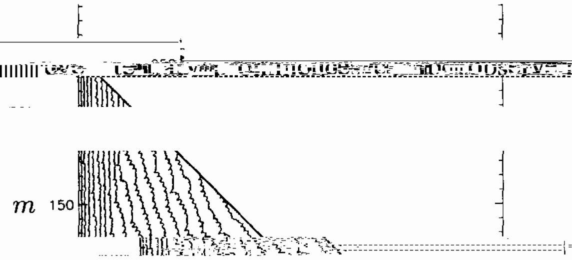

tremely important, and primary, secondary, and

that the Fourier coefficients have an extremely

coupling between the frequencies $\boldsymbol{\omega}$ appears to play the dominant role. Resonances gain and lose …

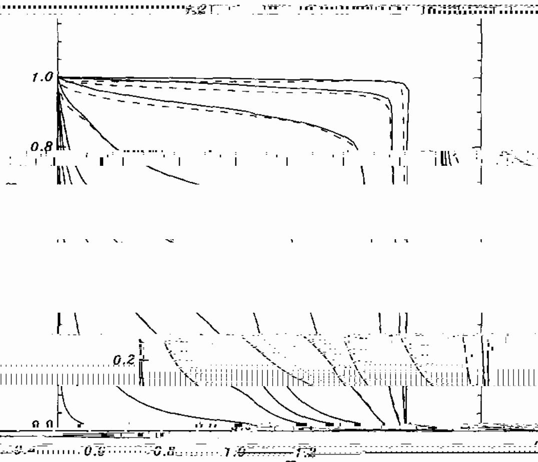

Fig. 4. Boundary of the domain of convergence for $\omega =$ ...

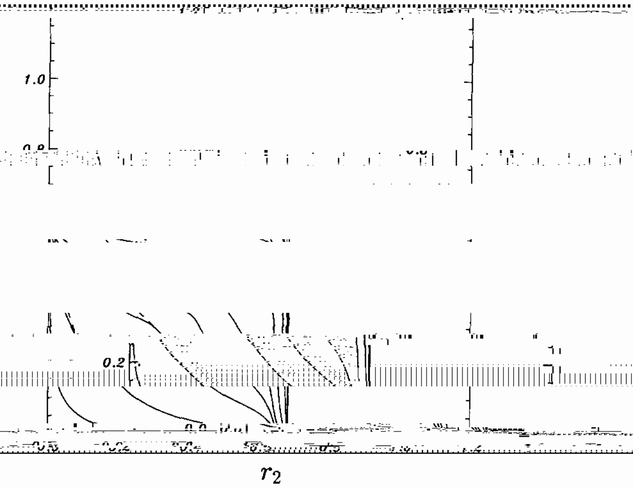

Fig. 6. Same as fig. 4 with $\omega = (\tau, \tau^2)$.

corresponds to the frequency $\omega_1 = \gamma$, and the horizontal to ...

frequencies. Note that the curves in figs. 4 and 6 ...

the r_2 axis occurs near 0.985, while table 1 implies that the correct value is 0.966. This overestimate is due to the fact that we compute the coefficients only out to the 255th Fourier ...

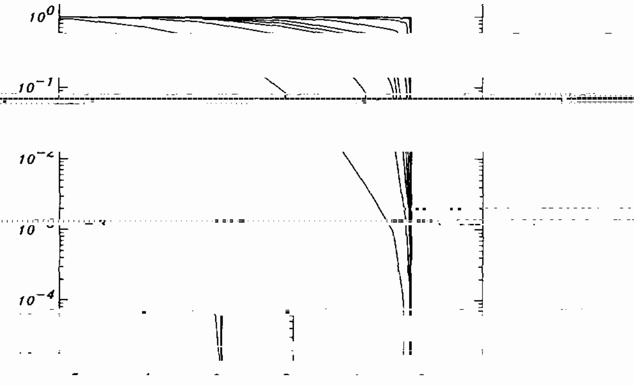

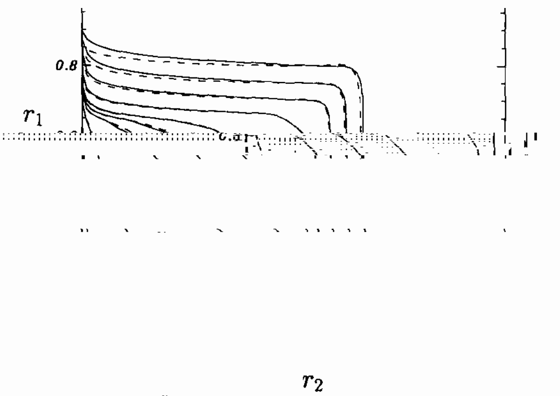

Fig. 5. Same as fig. 4 with $\omega = (\gamma, \zeta)$.

Table 1
Critical values for the semi-standard map.

$\gamma + \zeta$	0.00

ate evaluation of the critical function. For our

r. axis appears to be much lower than the value

actually rise rapidly to the correct (actually over-estimated) value as $r_2 \to 0$. It is interesting that in this case even through the values on axis are

$r_1^{(1)} = a^{ss}(\omega_1)$, independent of r_2; the numerical

limits to $a^{ss}(\omega_2)$ on the r_2 axis. This also occurs for the domain of convergence of the second

es, as shown in eq.

$$B_n^{(2)}(s) \simeq sk \frac{D_{(n,0)}}{D} b^{(1)}_{(n,0)} . \qquad (38)$$

(39)

bounded by the rectangle

scheme for finding $r_1(r_2)$ when k is small, we

Fig. 8 displays the coefficients $B_n^{(1)}$ and $B_n^{(2)}$ for $s = 10^{-25}$ and $\omega = (\gamma, \sigma)$. In the limit of small

spikes and valleys corresponding to a compli-

profile approaches a limiting form as $s \to 0$, even though the magnitude of $B^{(2)}$ approaches zero. Likewise, $B_n^{(2)}$ near the r_2 axis yields the semi-

to zero, while similarly converging to a fixed

rectangular domain for small k contains the do-

more quickly than for other ω curves, as we ...

for finding $r_1(s)$ has numerical problems when $k \ll 1$. For such small k, the singularity on one ... axis. To illustrate the problem consider a simple example which as a similar imbalance in the prominence of its singularities. Let

Here small values of δ simulate small values of k ... convergence of this series is the rectangle ...

We examine the behavior of eqs. (34)–(36) when applied to eq. (50) by a perturbation analysis near $s = 0$. For a finite n, the algorithm gives an error in r_1 of

$$\Delta r_1 \sim -\frac{\delta\alpha}{n}\left(\frac{\alpha s}{\beta}\right)^n . \qquad (51)$$

Thus the method works well provided ...

... switch to the inverse of the slope when $s = 1$. Thus, supposing $\beta < \alpha$ the method fails in a ...

below 10^{-5} in the computations.

... terms of the coupling parameter ϵ, instead of k. ... three dimensional graphs seen in figs. 9 and 10.

... sum frequency $\omega_1 + \omega_2$ through eq. (49). Numerical overflow for large k prevents us from calculating the curves for ϵ too close to its maximum value.

In many ways, it is these three-dimensional ...

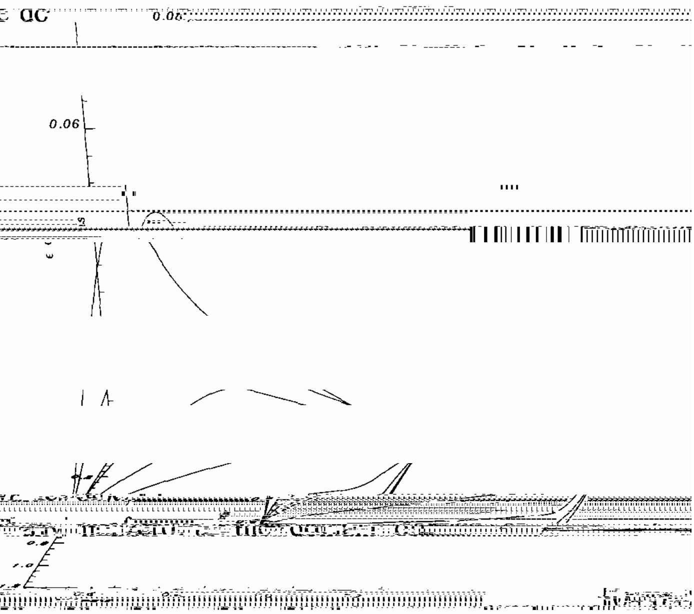

Fig. 9. Radii of convergence curves in ... for ... (σ) and $\omega = (\tau, \tau^2)$ where r_1 corresponds to the frequency τ, and r_2 to τ^2.

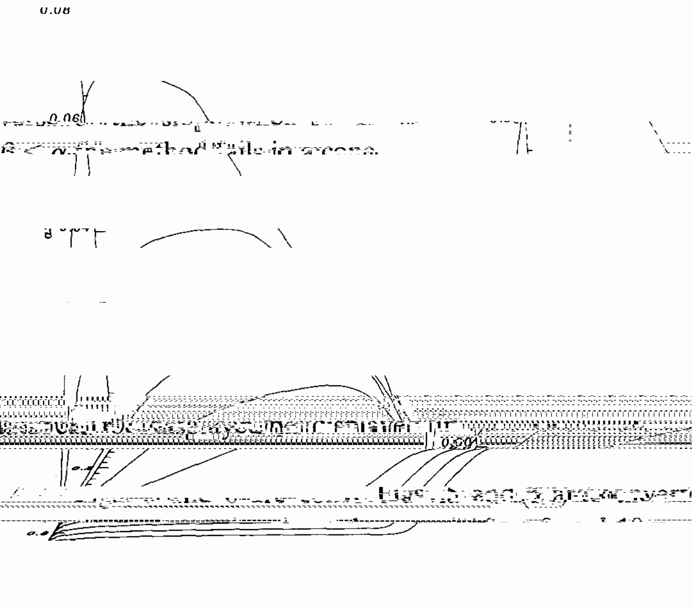

Fig. 10. Same as fig. 9 with ...

to determine the "last invariant torus". One

beginning at the origin. One could linearly order

definition of order.

Curve based order. An $\boldsymbol{\omega}$ torus persists longer than a $\boldsymbol{\mu}$ torus along a curve $\boldsymbol{\xi}(t)$ for which $\boldsymbol{\xi}(0)=\mathbf{0}$, if $\boldsymbol{\xi}(t)$ intersects the boundary of the domain of convergence of the $\boldsymbol{\mu}$ torus first.

The simplest example of a parameterized family

surface, which is all a curve based order allows. In some sense, one may want to incorporate the

torus persists longer than a $\boldsymbol{\mu}$ torus if the in-

If the surface is completely contained inside

the *partial ordering*

quencies will intersect in general, and then the

amples, the surface for (τ, τ^2) is completely con-

containment of the (γ, ζ) surface is partly due to

to compare the (γ, σ) and (γ, ζ) tori, note that though $a^{ss}(\sigma) > a^{ss}(\zeta)$, $a^{ss}(\gamma+\sigma) < a^{ss}(\gamma+\zeta)$. Thus the surfaces must intersect, and therefore there can only be parametrized comparisons.

Conclusions

We have determined the domain of existence

series in the angle variables. The semi-Froeshlé mapping has the advantage that two of the pa-

boundary of the domain for several frequency

be smooth, rather surprisingly. It appears smooth

when projected on the parameter

the uncoupled mappings. Furthermore, numerical results imply that the domain is bounded by

The methods and theorems of this paper are

ed [17]. They also apply to the 2d-dimensional

transition, J. Math. Phys. 20 (1979) 1183–1201.

[10] J.M. Greene and I.C. Percival, Hamiltonian maps in the

[11] J. Guckenheimer, B. Hu and J. Rudnick, Quasiperiodic Transition to Chaos with Three Incommensurate Fre-

mations in the study of dynamical systems, Phys. Rev. A

circles in area-preserving maps, Physica D 7 (1983) 283–300.

[16] R.S. McKay, On Greene's Residue Criterion, Universi-

(1992) 149–160.

tori for four-dimensional volume preserving maps, Nuovo Cimento 104B (1989) 177–183.

Tori of Cubic Irrational Winding Number, University of Houston (1989).

[25] M. Muldoon, Ghosts of Order on the Frontier of Chaos,

ones, Russ. Math. Surveys 32:6 (1977) 1–65;

G. Benettin, L. Galgani and A. Giorgilli, A proof of Nekhoroshev's theorem for the stability times in nearly

Physica D 6 (1982) 67–77.